Journal of Power Sources 196 (2011) 5133–5137

Contents lists available at ScienceDirect

Journal of Power Sources

journal homepage: www.elsevier.com/locate/jpowsour

Short communication

Synthesis of carbon-coated TiO_2 nanotubes for high-power lithium-ion batteries

Sang-Jun Park[a], Young-Jun Kim[b], Hyukjae Lee[a,*]

[a] Materials Research Center for Energy and Green Technology Andong National University Andong, Gyungbuk 760-745, South Korea
[b] Advanced Battery Research Center Korea Electronics Technology Institute Seongnam, Gyeonggi 463-816, South Korea

ARTICLE INFO

Article history:
Received 17 December 2010
Received in revised form 6 January 2011
Accepted 20 January 2011
Available online 3 March 2011

Keywords:
Anatase
Titania nanotubes
Carbon
Anode
Lithium-ion batteries

ABSTRACT

Carbon-coated TiO_2 nanotubes are prepared by a simple one-step hydrothermal method with an addition of glucose in the starting powder, and are characterized by morphological analysis and electrochemical measurement. A thin carbon coating on the nanotube surface effectively suppresses severe agglomeration of TiO_2 nanotubes during hydrothermal reaction and post calcination. This action results in better ionic and electronic kinetics when applied to lithium-ion batteries. Consequently, carbon-coated TiO_2 nanotubes deliver a remarkable lithium-ion intercalation/deintercalation performance, such as reversible capacities of 286 and 150 mAh g^{-1} at 250 and 7500 mA g^{-1}, respectively.

1. Introduction

As the demand for alternative electrode materials for Li-ion batteries is rapidly increasing, TiO_2 draws huge attention as an anode material due to its safety, abundance in nature, chemical stability, and non-toxicity [1,2]. The limitations of TiO_2 as an electrode material include its low Li-ion diffusivity and electronic conductivity which severely deteriorate reversible capacity and high-rate performance [3,4]. Nanostructuring of TiO_2 has been actively exploited to overcome these drawbacks by reduction of the transporting path for Li ions and electrons, and extension of the contact area between electrode and electrolyte. These effects have resulted in many significant successes [5–7].

Nonetheless, the intrinsically slow kinetics for both electrons and Li ions still hinder high-rate performance, which is an important factor for high-power applications. Hence, a nano-scale coating on the nanostructured TiO_2 has been attempted to improve the overall kinetics [8–15]. Depending on the material, the surface coating can promote faster Li-ion diffusion or electron transport, suppress the particle clustering frequently observed in nanoparticles, and/or limit excessive particle growth. Among various coating materials, carbon is the most widely used since it can improve the electronic conductivity of the non-conducting materials and be synthesized very easily using a variety of methods [12–15]. Unfortunately, the carbon coating on TiO_2 nanostructures has not been successful. Previous studies reported only marginal improvements in reversible capacity (up to 200 mAh g^{-1}) and in high rate capability from the carbon-coated TiO_2 nanostructures [12–15]. This may be because those studies focused primarily on an increase of electronic conductivity, which might not be sufficient to make a huge improvement on Li-ion intercalation performance, especially at high rates. Recently, several studies have shown that a non-conductive ceramic coating on TiO_2 nanotubes can significantly improve reversible capacity and high rate capability by suppression of the agglomeration and/or growth of TiO_2 nanotubes [8,9]. Better Li-ion intercalation performance is also expected if the carbon coating on TiO_2 nanotubes can act as a dispersant to limit agglomeration in addition to enhancing electronic conductivity. The present study aims to improve the Li-ion intercalation performance of TiO_2 by the carbon coating. As the first step, the ability of the carbon coating to suppress agglomeration of the nanotubes is investigated using carbon-coated TiO_2 nanotubes prepared by one-pot hydrothermal synthesis. Since the carbon coating can be easily prepared by a simple addition of a carbon precursor in the starting powder, it can have advantage in terms of simplicity and cost-effectiveness over other coating materials, which normally require additional steps for the coating.

2. Experimental

TiO_2 nanotubes were prepared by hydrothermal reaction of TiO_2 (anatase) powders with a NaOH aqueous solution [16]. For carbon-coated TiO_2 nanotubes, 1.5 g of glucose (Aldrich) and 4.5 g of TiO_2 powder (Aldrich) were dispersed in 75 mL of a 10 M NaOH (Aldrich) aqueous solution. After sonication in an ultrasonic

* Corresponding author. Tel.: +82 54 820 6272; fax: +82 54 820 6211.
E-mail address: hlee@andong.ac.kr (H. Lee).

0378-7753/$ – see front matter © 2011 Elsevier B.V. All rights reserved.
doi:10.1016/j.jpowsour.2011.01.105

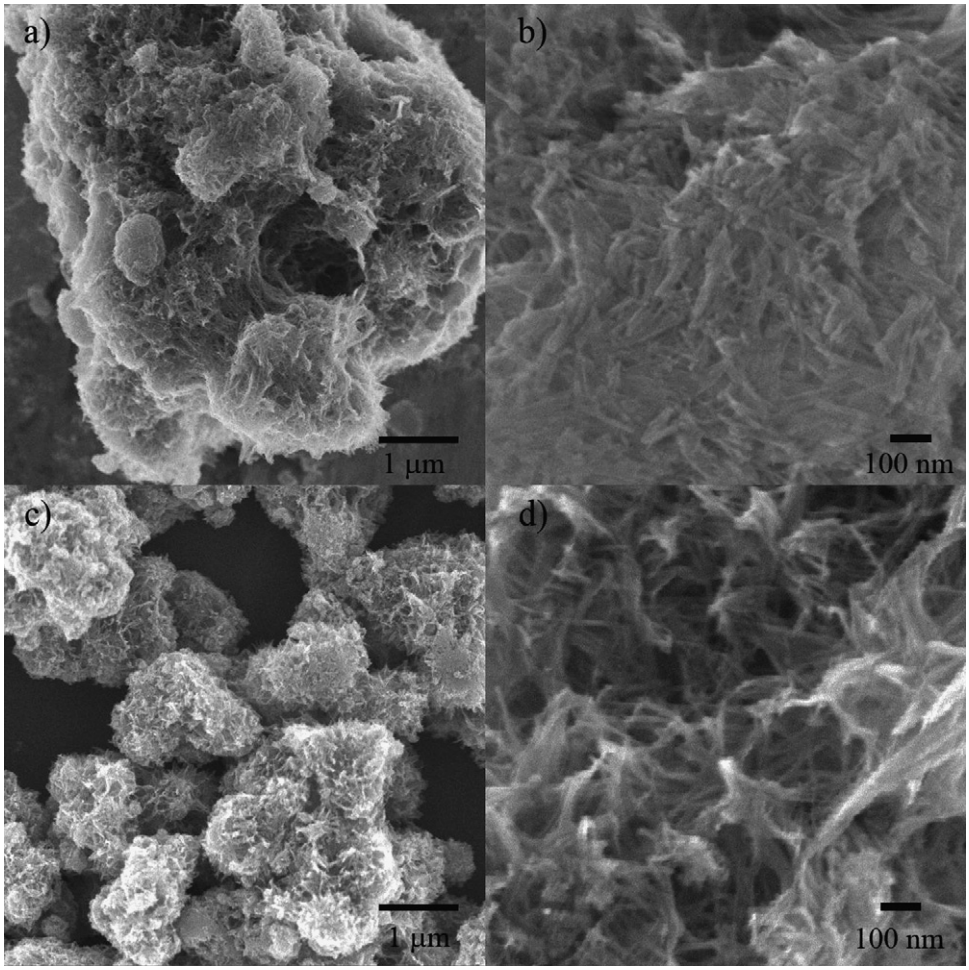

Fig. 1. SEM images of (a and b) PTNT and (c and d) CTNT.

bath for 30 min, the solution was transferred to a Teflon-lined stainless autoclave. Hydrothermal treatment was conducted at 180 °C for 3 h at the beginning and then at 150 °C for 48 h. The reaction product was washed with distilled water, a HCl solution (0.05 M), and distilled water until pH 7. For the pristine TiO_2 nanotubes, pure TiO_2 (6 g) was hydrothermally reacted in 75 mL of a 10 M NaOH aqueous solution at 150 °C for 48 h. After drying at 70 °C for 12 h, titanate nanotubes were calcined at 400 °C for 5 h in an argon-flowing tube furnace. Final products were examined by nitrogen adsorption isotherms (Micromeritics, ASAP-2010), X-ray diffraction (Rigaku, D/MAX 2000), elemental analysis (Fisons, EA 1108), scanning electron microscopy (JEOL, JSM-6700F), and transmission electron microscopy (JEOL, JEM-2010).

Coin cells (CR 2032) were constructed in a dry room to investigate Li-ion intercalation behaviour. The working electrode was prepared from 85 wt.% active material, 10 wt.% polyvinylidene fluoride, and 5 wt.% Super-P carbon black in a n-methyl-2-pyrrolidinone (NMP) solvent. The coin cells also used Li metal as a counter electrode, a Celgard 2400 as a separator, 1 M $LiPF_6$ in a mixture of ethylene carbonate (EC) and dimethyl carbonate (DMC) (1:1 in volume) as an electrolyte. The loading of all electrodes was about 1.7 mg cm^{-2}. The cells were galvanostatically charged and discharged over a voltage range of 1.0–3.0 V vs. Li^+/Li using a battery cycler (WonATech, WBCS3000). Electrochemical impedance spectroscopy (EIS) was conducted in the frequency range from 10^6 Hz to 1 mHz with an amplitude of 5 mV (PAR, Versastat3).

3. Results and discussion

For the sake of brevity, the pristine and carbon coated TiO_2 nanotubes will be denoted as PTNT (pristine TiO_2 nanotube) and CTNT (carbon coated TiO_2 nanotube), respectively. The SEM images show the effect of carbon coating on the clustering of nanotubes (Fig. 1). Without carbon coating, PTNT has a strong tendency to agglomerate and, consequently, forms secondary particles where individual nanotubes are tightly packed together. In some instances, several secondary particles are clustered together, resulting in very large aggregates as shown in Fig. 1a. This severe clustering of nanotubes prohibites direct access of Li-ion and electrons to the whole surface of the primary nanotubes and thereby annihilates the main benefit of nanostructuring. The added glucose appears to restrain extensive agglomeration by producing a thin layer of carbon on the nanotube surface. The SEM images of CTNT show somewhat loosely-attached individual nanotubes as compared with PTNT. In addition, the secondary particles appear to be evenly dispersed and the huge aggregate of secondary particles observed in PTNT is not found in CTNT. The TEM images (Fig. 2) show tubular morphology of TiO_2 nanotubes more clearly and no distinct morphological difference between PTNT and CTNT is observed probably due to the relatively low calcination temperature. TiO_2 nanotubes had inner diameters of 4–10 nm, outer diameters of 6–13 nm, and lengths of 60–300 nm. The densities of PTNT and CTNT determined by Archimedes' principle are 1.75 and 1.69 g cm^{-3}, respectively.

Due to the low calcination temperature, the crystallinity of TiO_2 nanotubes is rather poor and, therefore, XRD patterns (Fig. 3a) show

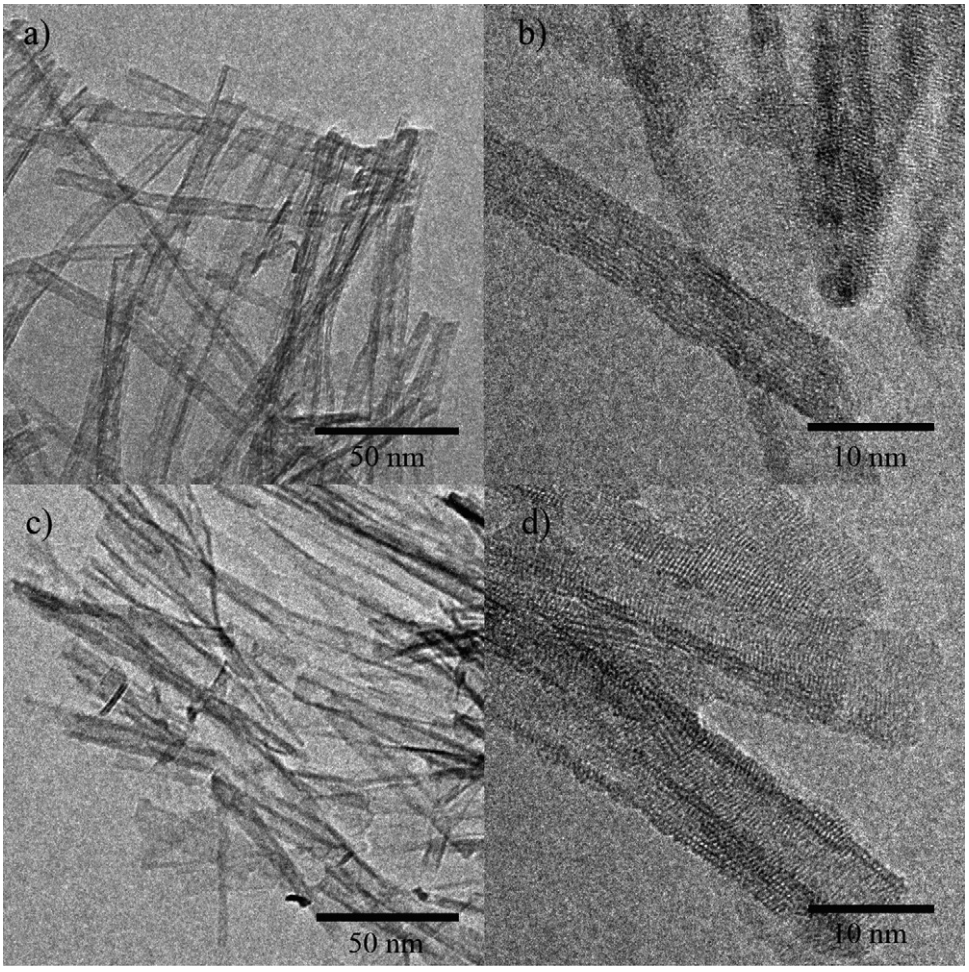

Fig. 2. TEM images of (a and b) PTNT and (c and d) CTNT.

weak anatase peaks. Indeed, the XRD pattern of CTNT displays even lower peak intensities which indicate that CTNT is more amorphous in nature. No other phase is identified in both PTNT and CTNT. Brunauer–Emmett–Teller (BET) surface areas are measured by nitrogen adsorption–desorption isotherms and, as expected, CTNT has a higher BET surface area because of its less tendency to agglomerate: 352 $m^2\,g^{-1}$ for CTNT and 315 $m^2\,g^{-1}$ for PTNT. Such a high surface area of CTNT makes it very difficult to detect the carbon layer on the nanotube surface in TEM images. In Fig. 2d, it is not possible to find the coated carbon layer on the surface of CTNT. Since the carbon content in CTNT measured by the elemental analysis is ~1 wt.%, the average carbon thickness can be estimated as ~0.02 nm based on the density of amorphous carbon (~1.8 $g\,cm^{-3}$) by assuming that the carbon is deposited evenly over the whole surface of the nanotubes. Although this calculation may not be realistic, it can give an insight into why it is impossible to observe the carbon coating under TEM.

The high surface area of CTNT can grant Li ions and electrons easy access to the whole surface of the nanotubes, resulting in the better kinetics for Li-ion intercalation/deintercalation. EIS measurements were conducted to elucidate Li-ion and electron kinetics in PTNT and CTNT electrodes. The Nyquist plots at open-circuit voltage of PTNT and CTNT are shown in Fig. 3b. They show a typical characteristic shape with a semi-circle in the high-frequency region connected with a straight line in the low-frequency region. The semi-circle at high frequencies corresponds to charge-transfer resistance at the electrode|electrolyte interface and the straight line at low frequencies represents a solid-state diffusion-controlled process of Li-ion [17]. The charge-transfer resistance of CTNT is lower than that of PTNT in Fig. 3b. Since the cell components and geometry are exactly same for both CTNT and PTNT, the lower charge transfer resistance of CTNT would be caused by the better electron and Li-ion kinetics due to the less-clustered nanotubes. It is noted here that the carbon coating from organic precursors should be heat-treated over 600 °C in order to improve the electronic conductivity of electrode materials [18]. Accordingly, the reduced charge transfer resistance of CTNT is attributed solely to the more open structured secondary particles.

Charge–discharge tests were conducted galvanostatically between 1 and 3 V (vs. Li^+/Li) at various rates from 250 to 7500 $mA\,g^{-1}$ and potential profiles at a rate of 250 $mA\,g^{-1}$ are shown in Fig. 4a and b. The potential profiles have a typical shape for anatase TiO_2, which consists of the plateau from two-phase intercalation followed by a sloping region that originates from supercapacitive behaviour. At 250 $mA\,g^{-1}$, the first reversible capacity of PTNT is 185 $mAh\,g^{-1}$, which is comparable to the values from other studies with similar synthetic and measurement conditions [16,19], and the reversible capacity at the 50th cycle is 179 $mAh\,g^{-1}$ with a capacity retention of 97%. Coulombic efficiencies are 95.8 and 99.1% at the first and 50th cycles, respectively. Carbon coating increases capacity substantially such that the first reversible capacity of CTNT is 285 $mAh\,g^{-1}$ (~54% increase in reversible capacity from PTNT). At the 50th cycle, the reversible capacity is still 273 $mAh\,g^{-1}$ (~53% increase from PTNT), i.e., a capacity retention of 96%. Coulombic efficiencies for CTNT are 98.7 and 99.4% at the first and 50th cycles, respectively. Not only are

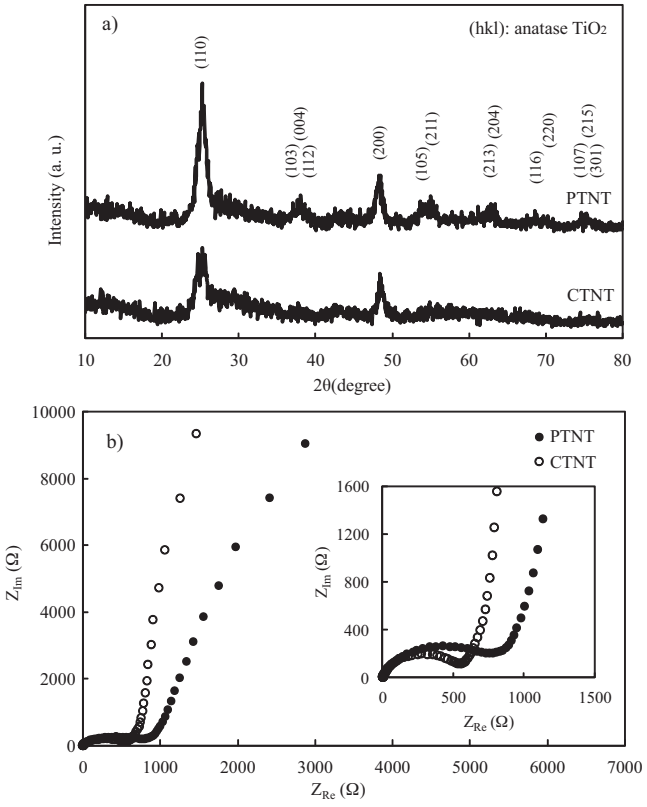

Fig. 3. (a) XRD diffraction patterns of PTNT and CTNT and (b) Nyquist plots from electrochemical impedance spectroscopy.

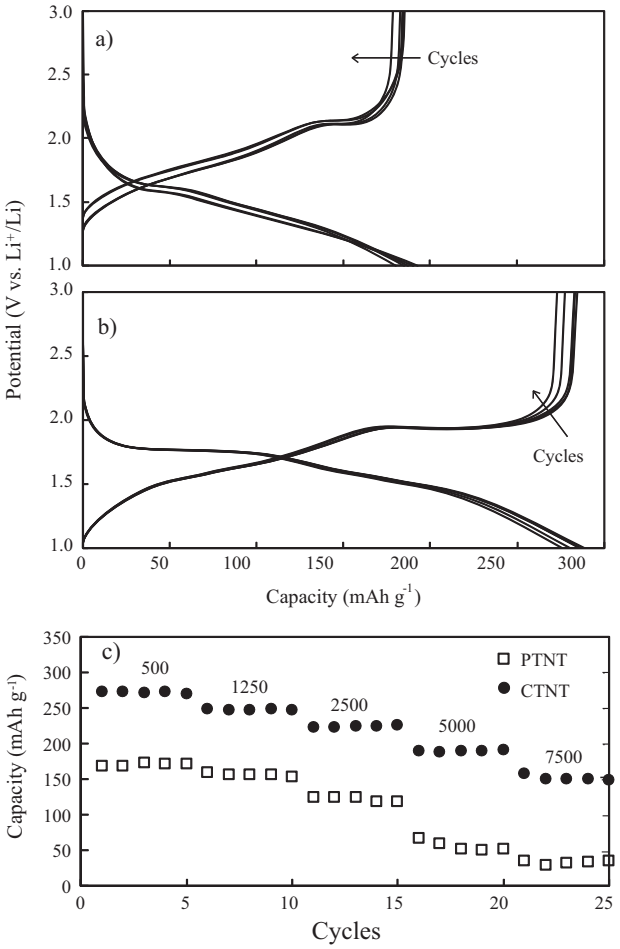

Fig. 4. Potential profiles at a rate of 250 mA g^{-1} for the 1st, 2nd, 10th, 20th, and 50th cycles for (a) PTNT and (b) CTNT. (c) Rate capabilities of TiO_2 nanotubes at rates of 500, 1250, 2500, 5000, and 7500 mA g^{-1}.

these values much higher than other reported capacities for carbon coated TiO_2 nanostructures (~140–200 mAh g^{-1}) [12–15], which were measured at even lower currents (60–200 mA g^{-1}) than those used in the present study (250 mA g^{-1}), but also they are higher than, or at least comparable with, the best results for TiO_2 anodes that have been reported previously (~220–270 mAh g^{-1}) [5,8].

Comparing potential profiles of PTNT and CTNT, CTNT has a longer plateau at 1.75 V, implying a more ordered phase transition from Li_xTiO_2 to $Li_{0.5}TiO_2$ [20]. This result appears surprising since CTNT shows a more amorphous nature in the XRD pattern (Fig. 3a) which normally results in a less resolved plateau for TiO_2. Nevertheless, both PTNT and CTNT have poor crystallinity, although PTNT showed relatively better crystallization, so that the degrees of crystallization of PTNT and CTNT may not be very different. If so, a better dispersion of nanotubes would be the reason for the pronounced plateau of CTNT since it could offer more accessible sites for the ordered phase transition. The better dispersion and the resulting high specific surface area of CTNT also leads to a substantial increase in supercapacitive capacity which is evident by the longer sloping region in the potential profile of CTNT as compared with that of PTNT. Although both PTNT and CTNT display high coulombic efficiencies, i.e., >99.1% at the 50th cycle, CTNT has a better cycling stability. In Fig. 4a, the potential profiles of PTNT display slight deviations between each cycle and the profile for the 50th cycle is quite different from that the first cycle. On the other hand, CTNT has almost identical potential profiles throughout all cycles and thus exhibits excellent cycling stability (Fig. 4b).

The discharge capacities of PTNT and CTNT at various rates (5 cycles for each rate) is given in Fig. 4c. The dramatic effect of the carbon coating at high rates is clearly addressed. The discharge capacities of PTNT at the 5th cycle are 153, 118, 51 and 36 mAh g^{-1} for discharge rates of 1250, 2500, 5000 and 7500 mA g^{-1}, respectively. These are only 81, 63, 27 and 19% of the discharge capacity at 250 mA g^{-1} (188 mAh g^{-1} at 5th cycle), respectively. Especially at 5000 mA g^{-1}, a large capacity drop from the capacity at 2500 mA g^{-1} can be seen in Fig. 4c, thus indicating very poor high-rate capability. Whereas PTNT suffers a large capacity loss at very high rates, CTNT exhibited good performance. At 1250, 2500, 5000 and 7500 mA g^{-1}, CTNT has a discharge capacity of 248, 226, 191 and 150 mAh g^{-1}, corresponding to 87, 79, 67 and 53% of the discharge capacity at 250 mA g^{-1} (285 mAh g^{-1} at 5th cycle), respectively. Comparing the discharge capacities at 7500 mA g^{-1}, it is clear that the high-rate capability, apart from the huge capacity improvement throughout the range of rates, is greatly enhanced by the carbon coating. Furthermore, the large capacity gap between 2500 and 5000 mA g^{-1} shown by PTNT (~67 mAh g^{-1}) is reduced by half with CTNT (~35 mAh g^{-1}). It is also important to mention that the working electrode has 85 wt.% of active material with only 5 wt.% of carbon black, whereas more than 10 wt.% of conducting agent is normally used in other studies [5–15]. Therefore, the Li-ion intercalation performance in the present study could be better if 10 wt.% of carbon black was used like other studies.

An important question is why other carbon coated TiO_2 nanostructures reported previously were not able to deliver an acceptable high-rate performance [12–15]. Most previous studies have focused on the improvement of electronic conductivity from the carbon coating, they have therefore failed to maintain a large surface area with a porous structure in the final product, because of the development of dense secondary particles via extensive aggregation, excessive growth of nanotubes during high

temperature calcination, etc. It is demonstrated that the high-rate capability of the ordered mesoporous TiO_2 is better than that of the metallized-disordered mesoporous TiO_2. This suggests that the access of electrolyte to the entire surface of TiO_2 is crucial to achieve a good high rate performance [5]. Unlike previous studies, the carbon coating in this study primarily acts as a dispersant to prevent severe agglomeration of TiO_2 nanotubes and, as a result, CTNT can deliver remarkable reversible capacities and high-rate capability. Similar Li-ion intercalation behaviour is also observed in TiO_2 nanotubes coated with ceramic stabilizers [8], but additional process steps are required for the ceramic coating, aside from the synthesis of TiO_2 nanotubes, and this may increase complexity and production cost. On the other hand, the use of an organic carbon precursor allows a simple one-step synthesis of carbon-coated TiO_2 nanotubes. In this study, the calcination temperature is 400 °C in order to minimize the agglomeration of nanotubes during heat treatment and exclude the effect of a change in electronic conductivity. On the other hand, it would be interesting to see if a carbon coating can improve the electronic conductivity of an TiO_2 anode while it acts as the dispersant simultaneously. This is a subject of ongoing research and the results will be addressed later.

4. Conclusions

Carbon-coated TiO_2 nanotubes are prepared by a simple one-step hydrothermal method with addition of glucose in the starting powder. A thin carbon-coating on the nanotube surface effectively suppresses severe agglomeration of TiO_2 nanotubes during hydrothermal reaction and post calcination, resulting in superior reversible capacity and high-rate capability. At 7500 mA g^{-1}, the gravimetric capacity of CTNT is ~150 mAh g^{-1}, which is about a threefold increase from that of PTNT. This study demonstrates that a high contact area between the electrolyte and the electrode, which is easily achieved by the carbon coating used in this study, is critical for improved reversible capacity and enhanced high-rate performance of TiO_2 nanotubes. In addition, the synthetic method in this work can also be applied to other polymorphs or nanostructural forms of TiO_2, such as TiO_2(B) nanowires, without any significant modification.

Acknowledgment

This work was supported by a National Research Foundation of Korea (NRF) grant funded by the Korean Government (MEST) (no. 2010-0022325).

References

[1] Z. Yang, D. Choi, S. Kerisit, K.M. Rosso, D. Wang, J. Zhang, G. Graff, J. Liu, J. Power Sources 192 (2009) 588–598.
[2] D. Deng, M.G. Kim, J.Y. Lee, J. Cho, Energy Environ. Sci. 2 (2009) 818–838.
[3] S. Bach, J.P. Pereira-Ramos, P. Willman, Electrochim. Acta 55 (2010) 4952–4959.
[4] D.V. Bavykin, J.M. Friedrich, F.C. Walsh, Adv. Mater. 18 (2006) 2807–2824.
[5] Y. Ren, L.J. Hardwick, P.G. Bruce, Angew. Chem. Int. Ed. 49 (2010) 2570–2574.
[6] Y. Wang, M. Wu, W.F. Zhang, Electrochim. Acra 53 (2008) 7863–7868.
[7] A.R. Armstrong, G. Armstrong, J. Canales, R. Garcia, P.G. Bruce, Adv. Mater. 17 (2005) 862–865.
[8] J. Jamnik, R. Dominko, B. Erjavec, M. Remskar, A. Pintar, M. Gaberscek, Adv. Mater. 21 (2009) 2715–2719.
[9] B. Erjavec, R. Dominko, P. Umek, S. Sturm, S. Pejovnik, M. Gaberscek, J. Jamnik, Electrochem. Commun. 10 (2008) 925–926.
[10] M. Mancini, P. Kubiak, M. Wohlfahrt-Mehrens, R. Marassi, J. Electrochem. Soc. 157 (2010) A164–170.
[11] M.G. Kim, H. Kim, J. Cho, J. Electrochem. Soc. 157 (2010) A802–A807.
[12] S. Yoon, B.H. Ka, C. Lee, M. Park, S.M. Oh, Electrochem. Solid-State Lett. 12 (2009) A28–A32.
[13] V.G. Pol, S.H. Kang, J.M. Calderon-Moreno, C.S. Johnson, M.M. Thackeray, J. Power Sources 195 (2010) 5039–5043.
[14] L.J. Fu, L.C. Yang, Y. Shi, B. Wang, Y.P. Wu, Microporous Mesoporous Mater. 117 (2009) 515–518.
[15] J. Xu, Y. Wang, Z. Li, W.F. Zhang, J. Power Sources 175 (2008) 903–908.
[16] J. Kim, J. Cho, J. Electrochem. Soc. 154 (2007) A542–A546.
[17] P.R. Bruno, E.R. Leite, J. Phys. Chem. B 107 (2003) 8868–8877.
[18] J. Moskon, R. Dominko, M. Gaberscek, R. Cerc-Korosec, J. Jamnik, J. Electrochem. Soc. 153 (2006) A1805–A1811.
[19] M.G. Choi, Y.G. Li, S.W. Song, K.M. Kim, Electrochim. Acta 55 (2010) 5975–5983.
[20] M. Marketa, M. Kalbac, L. Kavan, I. Exnar, M. Graetzel, Chem. Mater. 17 (2005) 1248–1255.